

# Protein-DNA Interactions Determine the Shapes of DNA Toroids Condensed in Virus Capsids

Amélie Leforestier,<sup>†</sup> Antonio Šiber,<sup>‡</sup> Françoise Livolant,<sup>†</sup> and Rudolf Podgornik<sup>§¶\*</sup>

<sup>†</sup>Laboratoire de Physique des Solides, Centre National de la Recherche Scientifique UMR 8502, Université Paris-Sud, Orsay, France;

<sup>‡</sup>Institute of Physics, Zagreb, Croatia; <sup>§</sup>Theoretical Physics Department, J. Stefan Institute, Ljubljana, Slovenia; and <sup>¶</sup>Institute of Biophysics, School of Medicine and Department of Physics, Faculty of Mathematics and Physics, University of Ljubljana, Ljubljana, Slovenia

**ABSTRACT** DNA toroids that form inside the bacteriophage capsid present different shapes according to whether they are formed by the addition of spermine or polyethylene glycol to the bathing solution. Spermine-DNA toroids present a convex, faceted section with no or minor distortions of the DNA interstrand spacing with respect to those observed in the bulk, whereas polyethylene glycol-induced toroids are flattened to the capsid inner surface and show a crescent-like, nonconvex shape. By modeling the energetics of the DNA toroid using a free-energy functional composed of energy contributions related to the elasticity of the wound DNA, exposed surface DNA energy, and adhesion between the DNA and the capsid, we established that the crescent shape of the toroidal DNA section comes from attractive interactions between DNA and the capsid. Such attractive interactions seem to be specific to the PEG condensation process and are not observed in the case of spermine-induced DNA condensation.

## INTRODUCTION

The control of DNA condensation plays a crucial role in both bacteria and eukaryotic cells at various stages of their cell cycle (1). DNA is tightly packed inside viral capsids (2) in densities almost approaching those of close packing. In an effort to unravel the mechanisms governing the condensation and decondensation processes at work in living cells, and given the difficulty of investigating the structure of these dense and complex DNA arrays without destroying them, investigators are focusing on simplified systems in which all parameters can be precisely controlled. DNA condensation can be reproduced *in vitro* and has been observed to undergo a drastic volume change upon addition of various condensing agents, including polyvalent cations such as polyamines (spermidine and spermine),  $\text{Co}(\text{NH}_3)_6^{3+}$ , polylysine, and histone H1, and even in the presence of monovalent cations with crowding agents such as polyethylene glycol (PEG) (3).

A most interesting case of DNA condensation is presented by DNA toroid formation, which can be observed under specific conditions such as very low DNA concentrations. Various images of toroids formed by multivalent cations and basic proteins can be found in the literature, and their characteristics and dimensions have been extensively discussed (4). By comparison, only a few micrographs of individual DNA chains collapsed by PEG have been presented (5,6), probably because of the preferred spherical or ellipsoidal conformation of the PEG-induced DNA globules (7). Ever since the DNA toroid was first observed, the regular and highly ordered form of the toroidal condensate has been attracting the interest of theorists (8,9). New cryo-electron microscopy (cryo-EM) methods have enabled a detailed, quantitative analysis of their internal

structure and explicit visualization of the local DNA ordering inside the toroid (10).

The formation of toroidal globules of single DNA chains trapped inside a confining volume was recently revealed by experiments in which the confining space was provided by a nanochannel (11), a liquid droplet (12), a liposome (13), or the virus capsid itself (14–16), either upon addition of spermine ( $\text{Spm}^{4+}$ ) or in a monovalent salt buffer containing PEG. These experiments raise additional theoretical and biological questions. DNA is always confined *in vivo*, regardless of the system under consideration. Each DNA chain, with its associated proteins forming chromatin, is confined in a chromosomal territory inside the nucleus of the eukaryotic cell (17), which is limited by the nuclear envelope. The bacterial nucleoid is confined in the central volume of the bacteria by the macromolecular crowding effect arising from other macromolecules (18), and the viral genome is confined within the protein capsid (19). This confinement is particularly important in the latter case because the capsid is rigid and entraps the entire genome under a very dense and as yet unknown conformation. Recent studies made it clear that after a partial ejection of the viral DNA, the fragment of the chain that is kept inside can be collapsed into a toroid (14–16). This transition between a confined coil and a confined toroid, triggered by changes in the environment of the virus, raises the question of how the capsid can influence the organization of the hedged-in DNA chain.

In this work, we focus on the formation of toroidal condensates of a single DNA chain inside an intact viral capsid, with corresponding DNA densities comparable to previous observations. We compare toroids formed by two different mechanisms: addition of  $\text{Spm}^{4+}$  or PEG to the outside bathing solution of the capsids. The toroidal DNA condensate can interact specifically with the confining capsid wall to the extent that its shape can be substantially modified by

Submitted January 24, 2011, and accepted for publication March 14, 2011.

\*Correspondence: rudolf.podgornik@fmf.uni-lj.si

Editor: Laura Finzi.

© 2011 by the Biophysical Society  
0006-3495/11/05/2209/8 \$2.00

doi: 10.1016/j.bpj.2011.03.012

this interaction. We observe this kind of strong DNA-capsid wall interaction only upon addition of PEG, which results in a drastic modification of the shape of the toroid. In comparison, the addition of spermine shows no modification in the shape of the DNA, indicating that there is only a weak interaction of the DNA toroid with the inner capsid wall.

## MATERIALS AND METHODS

### Biochemical purification

T5 st(0) bacteriophages were produced in *Escherichia coli*, purified, and concentrated at  $2.5 \times 10^{12}$  or  $5 \times 10^{12}$  phages/ml in 10 mM Tris-Cl<sup>-</sup> pH 7.6, 100 mM NaCl, 1 mM CaCl<sub>2</sub>, and 1 mM MgCl<sub>2</sub>. The protein receptor FhuA was purified as previously described (20) and stored at 4°C in 25 mM Tris-Cl pH 8.0, 250 mM NaCl, and 1% octyl glucoside (w:v) at a concentration of 4 mg/ml.

### Partial ejection and DNA condensation

Capsids containing only part of their genome were obtained either by freezing the specimen before the entire DNA molecule was ejected (time-resolved experiments (21)) or by applying an external osmotic pressure (34). The phage solution was mixed with an excess of FhuA (phage/protein ratio = 1:1000) in the absence or presence of an osmolyte (PEG, MW = 6000; Fluka, St. Louis, MO) and immediately transferred to 37°C to trigger the ejection. Lauryldimethylamine N-oxide (0.03%) was used to ensure the stability and solubility of the receptor protein. DNase I (Sigma, St. Louis, MO) was added at a concentration of 0.1 U/μl to digest the ejected DNA. The ejection was allowed to proceed for 10 min (absence of PEG) or 3 h (presence of PEG). Two alternative protocols were used to condense the DNA segment remaining inside the capsid: 1), addition of spermine at a final concentration of 5 mM (followed, when needed, by dilution of the sample to decrease the PEG concentration below 1% while keeping constant the ionic conditions); and 2), DNA ejection in the presence of 15% PEG 6000, followed by direct freezing of the sample in the PEG solution.

### Cryo-EM

A drop of the phage solution was deposited on an EM grid covered with a holey carbon film (Quantifoil R2/2) that was previously treated by plasma glow discharge. Grids were blotted to remove the excess material and immersed in liquid ethane cooled down by liquid nitrogen. The process was carried out with the use of an in-house-made plunging device to control the temperature and hygrometry, and to prevent any dehydration or any change of the ionic concentrations of the sample. The presence of PEG, which increases the viscosity of a solution and induces phage aggregation (visible at low magnification), made it more difficult to prepare thin films. The grids were transferred to a JEOL 2010 LaB<sub>6</sub> or a JEOL 2010-FEG transmission electron microscope operated at 200 kV. Images were recorded with a direct magnification of 50,000× under low-dose conditions (10–20 e<sup>-</sup>/Å<sup>2</sup>). The defocus was set at 850 nm to optimize the imaging of the DNA lattice spacing in the capsid.

## RESULTS

### Constrained DNA toroid formation inside viral capsids

T5 is a tailed bacteriophage that consists of a protein capsid hedging in the DNA genome, and a long tail through which

the double-stranded DNA chain is ejected upon interaction with the phage receptor inserted into the external membrane of the host bacteria (*E. coli*). The portal complex of the bacteriophage is located at one apex of the icosahedral capsid and connects the capsid to the tail. Using the protocols detailed in **Materials and Methods**, we prepared viruses whose capsids contained a single fragment of their initial genome of length  $L = 113.9$  kbp (38.7 μm). The length of the fragment varied from capsid to capsid and could only be determined a posteriori.

In Fig. 1 we present a selection of capsids containing a DNA fragment ~50–55,000 bp long (contour length ~17 μm). Depending on the preparation conditions used for the capsids, the DNA fragments could either occupy the entire volume of the capsid (Fig. 1 *a-a'*) or be condensed into toroidal globules (Fig. 1, *b-b'* and *c-c'*).

Fig. 1 *a'* shows a capsid immersed in a classical buffer (10mM Tris-Cl<sup>-</sup> containing monovalent salt (100 mM NaCl) with traces of divalent cations (1 mM MgCl<sub>2</sub> and 1 mM CaCl<sub>2</sub>) to maintain the integrity of the protein capsid. The DNA fragment obviously occupies the total volume of the capsid. From the estimated interhelical distance (~3.9 nm), we calculate the DNA concentration that falls within the range of the bulk cholesteric phase. Because the length of the encapsidated DNA cannot be controlled, it must be determined from the value of the interaxial spacing and the volume of the capsid itself. With the resolution of cryo-EM, we do not observe any specific interaction with the protein capsid under these particular conditions, i.e., we see no preferential adsorption to the surface or any significant exclusion from the peripheral volume close to the inner capsid wall. The DNA appears to be uniformly distributed within the entire capsid volume without any detectable variation in density (21). Concomitantly, we do not observe a pronounced depletion region with axial symmetry in the DNA density, which is sometimes predicted to exist on theoretical grounds (23). In fact, one could actually construct a robust theoretical argument that the axial depletion region should be quite small (24,25) and thus undetectable by the cryo-EM method.

The toroids presented in Fig. 1, *b-b'* and *c-c'*, were formed by collapsing a similar DNA fragment by adding either a tetravalent cation, spermine (Spm<sup>4+</sup>; Fig. 1 *b-b'*), or a neutral polymer (PEG; Fig. 1 *c-c'*) to the bathing solution of viruses while keeping all other solution conditions fixed. Details of the protocols used are given in the **Materials and Methods** section.

When polyvalent Spm<sup>4+</sup> cations, which are small enough to diffuse through the capsid wall, are added to the solution, they trigger the DNA coil–toroidal globule transition. As detailed in a previous study (26), DNA is hexagonally packed in the toroid and the interhelical distance ( $a_H$ ) is fixed by the balance of forces conferred by multivalent and monovalent cations. The measured value of the interaxial spacing under these conditions is  $a_H = 2.88 \pm 0.12$  nm. The polycations

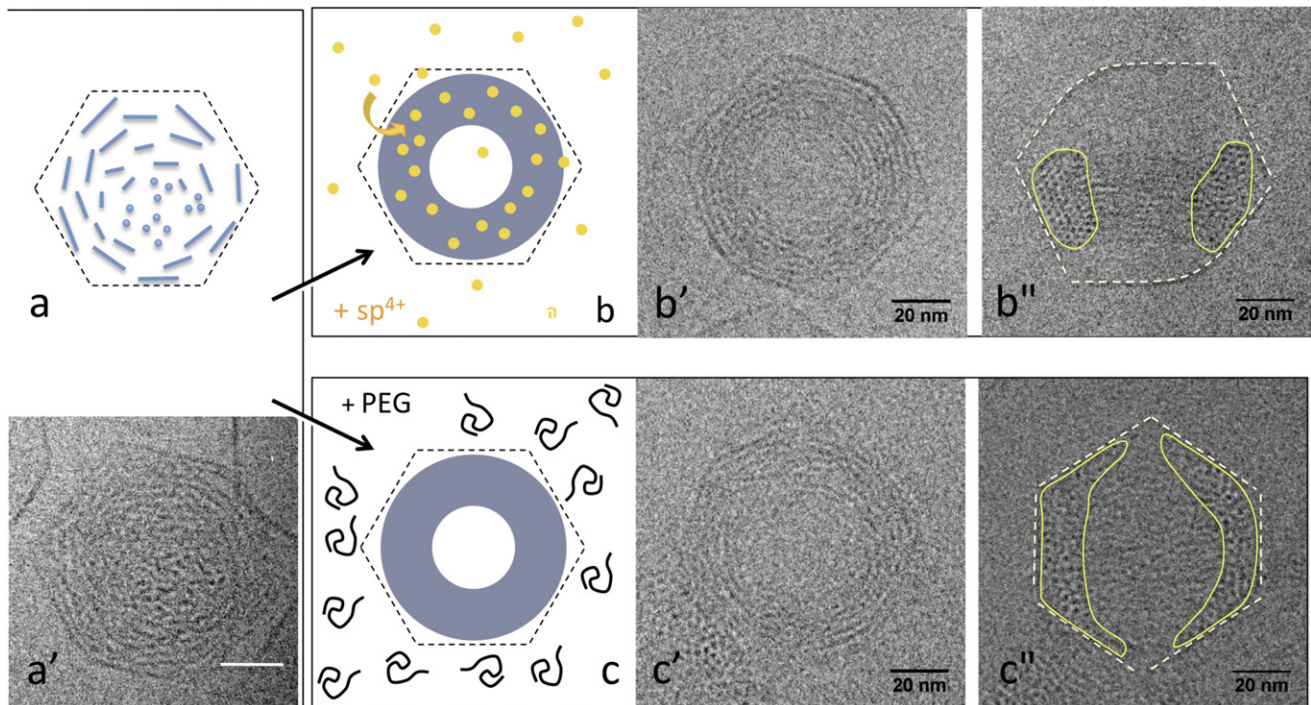


FIGURE 1 T5 bacteriophage capsids containing a double-stranded DNA fragment of  $\sim 17 \mu\text{m}$  (50,000 bp) after partial ejection of their genome. In the presence of monovalent cations (*a, a'*), the DNA chain occupies the entire volume of the capsid (*a'*). DNA toroids are formed by addition of polyamines ( $\text{Spm}^{4+}$ ) (*b-b''*) or PEG (*c-c''*) in the buffer. The polycations can go through the capsid, whereas PEG stays outside. For each condition, we present top (*b'* and *c'*) and side (*b''* and *c''*) views of the DNA toroids. The section of the toroid is shown with a contour on *b''* and *c''*. Scale bar = 20 nm.

provide the attractive component of the total force, whereas the monovalent counterions engender repulsive interactions. The balance of attraction and repulsion gives rise to a van der Waals-like behavior of the osmotic pressure (27,28) that at sufficiently high polyvalent cation concentrations leads to a minimum and an onset of condensation. The perpendicular section of the toroidal DNA globule often shows pronounced faceting that follows the reticular planes of the hexagonal lattice. As noted above, one of the reticular planes usually aligns itself parallel to the faces of the capsid (also shown in Fig. 1 *b''*). The external diameter of the toroid may be smaller than the diameter of the capsid (15), but the toroid nevertheless always sticks to the inner-wall capsid faces.

The formation of the DNA toroidal condensate presented in Fig. 1 *c'-c''* is due to the presence of PEG outside the capsid. PEG is well known to induce condensation of DNA in the presence of monovalent salts. This phenomenon is known as  $\psi$ -DNA condensation (29,30). The protein capsid behaves here as a semipermeable membrane that allows exchanges of water and ions from one side to the other while keeping the PEG and DNA separated. The protein capsid differs from a standard dialysis membrane in that it is rigid and does not deform under the osmotic pressure of PEG at the concentrations investigated. Indeed, the volume of the capsid stays roughly constant (within the resolution of our observations). The perpendicular section of the toroid in this case deviates significantly from a circle

and adopts a crescent-like shape with a markedly concave inner surface. This deformation of the cross section of the DNA condensate obviously increases the area of interaction between the DNA and the internal surface wall of the capsid. The local DNA packing is less regular in this case and shows an interaxial spacing of  $a_H = 3 \pm 0.2 \text{ nm}$ . At the concentrations used in the experiments (a 15% solution of PEG 6000), PEG exerts an osmotic pressure of, e.g., 3.2 atm (31). The capsids can withstand such an osmotic pressure without any trouble. In fact, osmotically induced elastic collapse of viral shells, as recently observed in the analogous case of frozen cationic lipid vesicles (32), occurs at larger values of osmotic pressure (typically  $>10 \text{ atm}$ ) in the case of empty viral shells (33) and at even higher values for DNA-filled capsids. These estimates, however, depend on the exact values of the elastic parameters used to characterize the capsid shell.

The experimentally observed shapes of the DNA condensates show variation for both  $\text{Spm}^{4+}$  and PEG condensation. One could argue that the temperature quench used in cryo-EM should show an equilibrium distribution of shapes corresponding to the free energies of the different shapes. If there were a well-defined ground state of minimal energy separated from other shapes by a finite energy gap, one could expect this ground-state shape to dominate the observed shape space spectrum. The broadness of this spectrum, on the other hand, would indicate that relatively

different shapes share similar free energies and should thus show up in the quenched distribution provided by cryo-EM. The experiments typically do not show noncrescent-like shapes in the case of PEG condensation, and thus our singling out of this shape as a consequence of the pronounced attractive DNA condensate-capsid wall interactions seems to carry some weight.

We want to make it clear that here we are not studying how the presence of PEG outside the capsid interacts with the ejection mechanism itself. Rather, we are focusing on capsids that contain a fragment of their initial DNA genome, mimicking capsids at an intermediate state of DNA encapsidation or ejection. PEG has previously been used to oppose the ejection of DNA from the capsid of  $\lambda$ , T5, and Spp1 bacteriophages. In contrast to  $\lambda$  (34) and Spp1 (35), in which the fraction of ejected DNA is directly related to the applied pressure, in T5 one cannot control the remaining encapsidated length of the DNA by varying the external osmotic pressure (22). The mechanism is more tricky and is not fully elucidated, and for each applied pressure capsids are found that contain varying amounts of encapsidated DNA. One can also prepare incompletely filled capsids without any osmotic pressure opposing the ejection, just by stopping the ejection before its completion (21).

### Theory of a DNA toroid constrained in a sticky sphere

In these experiments, we are investigating a very complicated situation involving multiple interactions. It is almost hopeless and probably not very useful to approach the problem by microscopic representation of all the involved entities and interactions. Therefore, we simplify the situation by modeling the condensed DNA toroid using a continuum theory that accounts for the elastic energy of the wound-up DNA ( $F_{el}$ ), the energy of the exposed surface of the toroid ( $\sigma A$ , where  $\sigma$  is the effective surface tension of the unconstrained DNA toroid and  $A$  is its surface area), and an attractive adhesion energy of the toroid-capsid interaction. The free energy functional of our model is

$$F = \sigma A + F_{el} - \sigma_a A_a \quad (1)$$

where the first two terms (the surface free energy of the toroid, and the elastic energy of the wound-up DNA) are the same as in the model proposed by Ubbink and Odijk (36). The third term complicates the model and makes it less tractable due to the introduction of a surface energy parameter,  $\sigma_a$ , that depends on the strength of the effective short-range DNA-capsid interaction. The area of the contact region between the DNA condensate and the inside capsid wall is denoted by  $A_a$ . This is an unknown quantity whose value is obtained only after the minimization of the functional. We consider the free-energy functional on a hyperplane of constant DNA volume,  $V$ , the same as in the Ubbink-Odijk (UO) model. In our case, we additionally

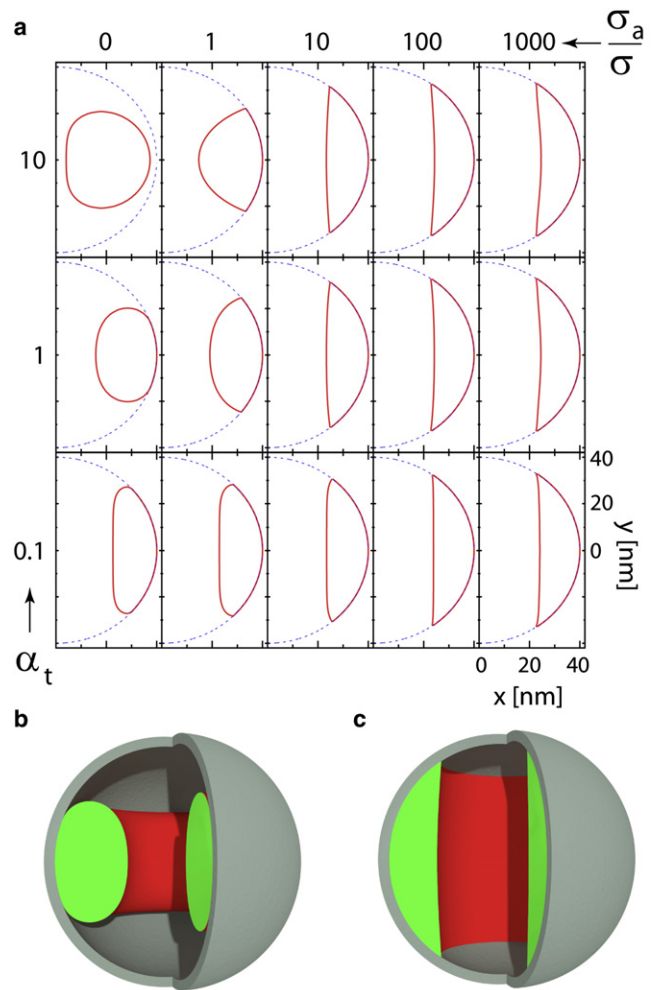


FIGURE 2 (a) Shapes of DNA toroids in  $[\alpha_t, \sigma_a/\sigma]$  parameter space. Blue dashed lines indicate the inner surface of the spherical container with  $R = 40$  nm. The volume of the DNA in these calculations was fixed to  $V = 1.4 \cdot 10^5 \text{ nm}^3$ . (b) Three-dimensional rendering of the DNA toroid with  $\alpha_t = 1$ ,  $\sigma_a/\sigma = 0$ . (c) Three-dimensional rendering of the DNA toroid with  $\alpha_t = 10$ ,  $\sigma_a/\sigma = 100$ .

restrict the problem by the introduction of the capsid, which acts as a constraint, allowing only solutions contained within the sphere of radius  $R$ .

In the UO model, the solution for the shape of the DNA toroid depends on only two parameters: the volume  $V = l^3$  and an adimensional parameter  $\alpha_t$  that weights the relative importance of the surface and elastic energies:

$$\alpha_t = \frac{2\sigma l^4}{LP} \quad (2)$$

where  $L$  and  $P$  are the contour and persistence lengths of the DNA, respectively, and  $l$  is defined above in terms of  $V$ . In our case, the solution also depends on the ratios  $R/l$  and  $\sigma_a/\sigma$ . When  $R/l = \infty$ , corresponding to an unconstrained torus inside an infinitely large capsid, and  $\sigma_a/\sigma = 0$ , our model reduces to the one studied by Ubbink and Odijk

(36), and we verified that this is indeed so by examining our results in this limit. The experiments restrict the freedom of our theoretical model because they fix the constraint (capsid) radius and the DNA volume. The DNA volume and the radius of the capsid interior can be obtained from experimental images of phages (see Fig. 1). In this way, we determine  $V = 1.4 \cdot 10^5 \text{ nm}^3$  (with an interhelical distance equal to 3 nm and a basepair separation of 0.34 nm, this corresponds to  $L = 53 \text{ kbp}$  and  $R = 40 \text{ nm}$ ).

Although faceting in the perpendicular cross section of the DNA condensate can sometimes be observed in our experiments, the continuum UO model (or any continuum model for that matter) does not take into account the discrete nature of the DNA lattice within the condensate and thus cannot account for discrete features such as toroid faceting. Formally, the faceting is an effect of the orientational dependence of the surface energy ( $\sigma$  in our case), which we assume to be a constant, and can be obtained via a Wulff construction, such as in the theory of equilibrium shapes of crystals (37). In a similar vein, we also do not take into account the polyhedral structure of the capsid wall or its discrete protein architecture, and instead treat it as being ideally and uniformly spherical. The inner polyhedral faces can in fact promote a preferred interaction between the facets of the DNA condensate and the centers of the polyhedral faces, leading to preferred connected interaction patches along the inner capsid surface.

### Numerical analysis of the model

For comparison with experiments, we examine the model on a remaining two-dimensional plane of (unknown) parameters,  $\alpha_t$  and  $\sigma_a/\sigma$ . The toroid shapes are fully determined by their cross sections. These are first represented in a discrete form, i.e., by  $N$  points, where  $N$  is typically of the order of 500. Only half of the cross section needs to be represented; the other half can be obtained by reflection. The free-energy functional is then represented in terms of the coordinates of these points, so that it becomes a function of  $N$  variables. This function is numerically minimized by using a suitable variant of the conjugate gradient optimization. The constraints of the fixed volume and the impenetrable capsid wall are implemented via energy-penalty contributions to the functional. The inclusion of the short-range attraction in the functional requires a specification of the critical separation between the toroid patch and the surface. Below the critical separation, the toroid patch is considered to be in contact with the capsid, and only then does its area contribute to the total area of the contact region,  $A_a$ . The critical separation should be made as small as possible to ensure that it is by far the smallest length in the model and that the solutions do not depend on its exact choice.

A shape phase-diagram of the problem representing the optimal toroid cross sections for a particular combination

of  $\alpha_t$  and  $\sigma_a/\sigma$  parameters is shown in Fig. 2. Cross sections corresponding to the  $\sigma_a/\sigma = 0$  case, i.e., without attraction between the DNA and the capsid, are presented in the first column of images in Fig. 2 a. Note that the top-left shape ( $\sigma_a/\sigma = 0$  and  $\alpha_t = 10$ ) is the same as would be obtained in the UO model, because the toroid does not touch the capsid in this case, i.e., the capsid impenetrability constraint is not active. (One might wonder whether there is a need to examine the behavior of the model for negative values of the  $\sigma_a/\sigma$  ratio. This would correspond to repulsion between the DNA and the capsid. However, for short-ranged repulsions, this would simply result in an effective renormalization of the constraint radius, i.e., an appearance of the void spherical shell between the toroid and the capsid whose thickness  $d$  would correspond to the effective range of the repulsion. The toroid would thus behave as constrained in a sphere of radius  $R - d$ .) For a sufficiently large adhesion energy parameter (the last column of images in Fig. 2 a), the cross section of the DNA toroid only weakly depends on  $\alpha_t$ . Obviously the presence of attractive interactions between the capsid wall and the toroidal condensate leads to a deformation of its cross section that becomes markedly concave and crescent-like (Fig. 2 c). For the values of the  $\sigma_a/\sigma$  ratio, the set of parameters determined by the DNA volume and the capsid radius indicated in Fig. 2 a, the concaveness of the cross section is effectively saturated and any further increase in this ratio leads only to insignificant changes.

By analyzing numerical solutions for very small values of the  $\alpha_t$  parameter, without any attraction between the capsid wall and the DNA toroid ( $\sigma_a/\sigma = 0$ ), we find that the limiting shape for small values of  $\alpha_t$  is a plan-convex lens. This leads to the conclusion that the concavity of the inner surface of the DNA toroid section can be observed only when the attraction between the DNA and the capsid is present. Otherwise, the cross sections are always flat or convex, i.e., the shape constraint in combination with elasticity and the surface energy minimization cannot produce a concave shape. The crescent-like form of the condensate cross section thus appears to be the distinguishing feature of the attractive interaction between the DNA condensate and the capsid wall.

The experiment shows two markedly different types of toroid shapes (Fig. 1). In numerical calculations, the characteristic crescent-like shapes of the cross sections with concave inner surface (Fig. 2), which are similar to those found in experiments with PEG, are obtained only in the case of a sufficiently strong attractive interaction between the DNA condensate and the inner capsid wall as codified by the parameter  $\sigma_a/\sigma$ . These distinguishing features are certainly observed in the case of PEG condensation, but are absent in the case of Spm<sup>4+</sup> condensation. In the latter case, one can identify more circle-like cross sections consistent with model calculations for  $\alpha_t \sim 1$  and sufficiently small  $\sigma_a/\sigma < 1$ .

The comparison of the model with the experiments thus suggests that the system has quite different energetics

when the solution contains PEG and  $\text{Spm}^{4+}$ .  $\text{Spm}^{4+}$  ions apparently condense DNA and do not induce significant DNA-capsid attraction, whereas PEG molecules do, although the capsid is impermeable to them.

## DISCUSSION

There are a few features of our results regarding DNA condensation in capsids that we need to put in perspective.

It follows from our observations and the corresponding model analysis that the strength of DNA toroid-capsid wall interactions is much larger in the case of PEG condensation than in the case of  $\text{Spm}^{4+}$  condensation. In the latter case, there is a tendency for the (faceted) condensate as a whole to interact with the capsid surface, or more correctly with its polyhedral faces, but this surface interaction does not appear to be large enough to deform the shape of the condensate. This interaction can become substantial when the toroid outer radius is larger than the inner radius of the capsid. In that case, the confinement interaction of the DNA toroid that is forced to reside inside the capsid dominates (38), but the confinement alone, without any attractive interactions between the DNA condensate and the capsid wall, can only modify the shape of the toroidal condensate in such a way that the inner surface of the condensate becomes flat and remains so (in the limit when  $\alpha_t \geq 0$ ) while the outer surface is pushed against the inner surface of the capsid. Thus, confinement in and of itself cannot simulate attractions between the DNA condensate and the capsid wall.

The model that is used to analyze the possible shapes of a confined toroidal condensate, with or without surface-specific interactions with the confining wall, is based on three effective parameters:  $\alpha_t$ ,  $\sigma_d/\sigma$ , and the effective radius of the capsid. All of the numerical results presented above depend on the combination of these three parameters characterizing the model of the confined DNA toroidal condensate. Short-range microscopic interactions between capsid wall protein moieties and DNA are clearly the dominant contribution to the  $\sigma_d/\sigma$  ratio. At least in part, these interactions have to be electrostatic in nature, as both DNA and capsid proteins contain many charges, but more specific protein binding to DNA cannot be excluded. The  $\alpha_t$  parameter obviously depends on whatever interactions set the equilibrium spacing between the DNA molecules in the condensate, as well as the elasticity and total length of the molecule. The surface tension of the DNA toroid can also be modified by the condensing agent, and probably is. The attractive branch of these interactions is generally assumed to be due at least in part to an electrostatic correlation effect (39), but it should also depend on the specific properties of the polyvalent condensing agents (40,41) because even equally charged condensing cations do not induce DNA condensation to the same extent. The specific properties of ions that differentiate different types of DNA condensing cations are relatively

poorly known and still inadequately understood (42). The two parameters of the continuum model that guided our analysis of the PEG- and  $\text{Spm}^{4+}$ -induced DNA condensation in vitro can be estimated very roughly to be  $\alpha_t \sim 1$  and  $\sigma_d/\sigma \sim 0$  for the  $\text{Spm}^{4+}$ -induced aggregation and concurrent shape of the confined DNA toroidal, whereas  $\alpha_t \sim 1$  and  $\sigma_d/\sigma \sim 100$  would be more appropriate for the PEG-induced aggregation.

What are the physical reasons for the fundamental difference between PEG and  $\text{Spm}^{4+}$  in the observed behavior of DNA condensation induced in capsids? The experiment itself does not give a definitive answer to this question. Nevertheless, we can try to patch together a string of arguments that may shed some light on this problem. PEG itself does not induce a direct interaction between DNA segments. In fact, in DNA condensation experiments that are based on long fragments of DNA, DNA and PEG spontaneously demix. What PEG always induces is a modification in the chemical potential of water, implying that the properties of water inside the capsid are changed, and that its chemical potential adjusts to the same new value that is set by the concentration of PEG in the bathing solution. Once the chemical potential of the water inside the capsid is changed, the DNA self-condenses to counter this new value of the chemical potential or (in what amounts to the same thing) the osmotic pressure. The fact that the state of the DNA depends on the water chemical potential or its osmotic pressure was amply demonstrated in experiments by Rau and Parsegian (27), who induced DNA condensation directly by changing the PEG concentration in the bathing solution. One should realize that in their study, the DNA subphase and the bathing solution were sometimes separated by a semipermeable flexible membrane. In our experiments the membrane was rigid, but we do not think that this invalidates our argument. The same is true here, as the DNA interhelix distance decreased from  $\sim 3.9$  nm to 3 nm after addition of PEG. The chemical potential of water in the PEG bathing solution thus sets the chemical potential of water inside the capsid, and the DNA reacts to this change by condensing. The PEG-induced condensation appears quite different from the  $\text{Spm}^{4+}$ -induced condensation, where the condensing agent gives rise to explicit attractive interactions between DNA molecules that can be rationalized as being mediated either by attractive electrostatic correlation interactions (43) or by attractive hydration interactions (27) that lead to condensation. The main difference between the PEG-induced and the polyvalent counterion-induced condensation of DNA would thus be the indirect versus direct routes to DNA condensation.

The main difference between our PEG experiments and those of Rau and Parsegian (40) is that in our case, the semipermeable capsid was rigid. The consequence of this rigidity is that the volume of the capsid is kept, to a good approximation, a constant. Therefore, the collapsed DNA occupies only a fraction of the capsid volume, and two compartments are created inside the capsid: one containing DNA with its

associated water and counterions, and one devoid of DNA. In their experiments, Rau and Parsegian (40) generally used no semipermeable membrane, and therefore there were only two compartments: the DNA solution and the PEG solution. The existence of the third compartment could possibly be a consequence of the negative hydrostatic pressure inside the capsid caused by its impenetrability to the external PEG, but we cannot say anything more definitive at this point. We thus leave the PEG-induced condensation in capsids as a challenge for the theory.

Our results could also have broader ramifications when considered together with some other related experimental investigations. One might wonder whether the formation of toroids, which has been only exceptionally reported in the bulk in the presence of crowding agents (5), is facilitated by confinement inside the capsid. Zhang et al. (11) recently observed that confinement of the DNA chain in a nanochannel facilitates compaction with a neutral crowding agent at low ionic strength. The observation by Hou et al. (12) that toroids can be formed inside confined droplets adsorbed on mica surfaces solely by geometric confinement, and in the absence of any condensing agent, would further support such a hypothesis. Additionally, one might also wonder whether DNA condensation is assisted and directed by the internal surface of the capsid itself, as is apparently the case for a mica surface (44) or the phospholipid membrane of a giant vesicle (45).

It appears that PEG, via changes in the water chemical potential or its osmotic pressure, can not only induce DNA aggregation but also effect conformational changes in the proteins of the capsid wall. This assertion is of course speculative, since we do not have any direct indications that it is true. Nevertheless, we know that as a result of its effect on the chemical potential of water, PEG can effect conformational changes in hemoglobin and various membrane (channel) proteins (46). Therefore, it is not preposterous to hypothesize that PEG could also affect the conformation of capsid proteins, which in turn could lead to a more pronounced interaction with the DNA. This interaction can again be either very specific or quite generic (i.e., electrostatic). It would be difficult to assert more at this point, but it is possible that a separate investigation of the conformation of capsid proteins as a function of PEG osmotic pressure could settle some of the subtler points of our speculation.

Currently, the exact distribution of charges on a protein surface interacting with DNA remains unknown because the structure of the capsid has not been solved yet. Nevertheless, it is known that T5, like  $\lambda$  and HK97, belongs to the Siphoviridae family of viruses. The structure of the capsid has been elucidated at atomic resolution only for HK97 (47). The proteins pb8 (the main component of the T5 capsid) and gp5 (which constitutes the capsid of HK97) share sequence similarities as well as the same fold (except for some loops involved in the HK97 interlinked rings (catenanes)) (48). We can thus rely on HK97 to give us an idea of the distribution

of amino acids (and charges) on the internal surface of the T5 capsid. A few positive charges could favor attractive interactions with the encapsidated DNA together with a comparable number of negative charges that may also constitute possible loci for electrostatic links to the negative DNA phosphate charges through the intermediate bridging of divalent cations that are present (and required) in the buffer.

Regardless of the details of this PEG-induced attractive interaction between DNA and the capsid, it is clear that the condensation of DNA in capsids onto the internal protein surface creates an empty space in the center of the capsid. This effect should also exist in newly synthesized capsids inside the bacteria. The highly crowded condition of the bacterial cytoplasm should favor condensation of the entering DNA into the capsid (as did PEG in our experiments) and provide an empty space in the center of the capsid, thus supporting the encapsidation process and facilitating the work of the portal motor.

We thank Gerard Pehau-Arnaudet (Institut Pasteur, Paris) for his help with the federative FEG microscope, and Madalena Renouard (Institut de Biochimie et Biophysique Moléculaire et Cellulaire, Orsay, France) for the biochemical purification of bacteriophage T5 and its protein receptor PhuA. We also thank M. Castelnovo for drawing F.L.'s attention to the likely presence of toroids in Fig. 5 of Leforestier and Livolant (15). F.L. and R.P. thank the Aspen Center for Physics for hosting the workshop on Filamentous Assemblies: Complex Ordering from Biopolymers to Nanorods (2009), organized by G. M. Grason, R. F. Bruinsma, and J. M. Schwarz, which gave rise to the ideas presented in this work.

This study was supported funds from the Agency for Research and Development of Slovenia (grant P1-0055(C)) to R.P., and the Ministry of Science, Education, and Sports of Republic of Croatia (project No. 035-0352828-2837) to A.Š.

## REFERENCES

1. Wolffe, A. P. 1998. Chromatin structure. *Advances in Genome Biology*. 5:363–414.
2. Cerritelli, M. E., N. Cheng, ..., A. C. Steven. 1997. Encapsidated conformation of bacteriophage T7 DNA. *Cell*. 91:271–280.
3. Bloomfield, V. A. 1996. DNA condensation. *Curr. Opin. Struct. Biol.* 6:334–341.
4. Hud, N. V., and I. D. Vilfan. 2005. Toroidal DNA condensates: unraveling the fine structure and the role of nucleation in determining size. *Annu. Rev. Biophys. Biomol. Struct.* 34:295–318.
5. Evdokimov, Y. M., A. L. Platonov, ..., Y. M. Varshavsky. 1972. A compact form of double-stranded DNA in solution. *FEBS Lett.* 23:180–184.
6. Evdokimov, Y. M., T. L. Pyatigorskaya, ..., Y. M. Varshavsky. 1976. A comparative X-ray diffraction and circular dichroism study of DNA compact particles formed in water-salt solutions, containing poly(ethylene glycol). *Nucleic Acids Res.* 3:2353–2366.
7. Laemmli, U. K. 1975. Characterization of DNA condensates induced by poly(ethylene oxide) and polylysine. *Proc. Natl. Acad. Sci. USA*. 72:4288–4292.
8. Grosberg, A. Yu., and A. V. Zhestkov. 1986. On the compact form of linear duplex DNA: globular states of the uniform elastic (persistent) macromolecule. *J. Biomol. Struct. Dyn.* 3:859–872.
9. Ubbink, J., and T. Odijk. 1996. Deformation of toroidal DNA condensates under surface stress. *Europhys. Lett.* 33:353–358.

10. Hud, N. V., and K. H. Downing. 2001. Cryoelectron microscopy of phage  $\lambda$  condensates in vitreous ice: the fine structure of DNA toroids. *Proc. Natl. Acad. Sci. USA.* 98:14925–14930.
11. Zhang, C., P. G. Shao, ..., R. C. van der Maarel. 2009. Macromolecular crowding induced elongation and compaction in a nanochannel. *Biophys. J.* 97:1678–1686.
12. Hou, X.-M., W. Li, ..., P. Y. Wang. 2009. Formation of DNA toroids inside confined droplets adsorbed on mica surfaces. *Phys. Rev. E Stat. Nonlin. Soft Matter Phys.* 79:051912.
13. Lambert, O., L. Letellier, ..., J.-L. Rigaud. 2000. DNA delivery by phage as a strategy for encapsulating toroidal condensates of arbitrary size into liposomes. *Proc. Natl. Acad. Sci. USA.* 97:7248–7253.
14. Evilevitch, A. 2006. Effect of condensing agents and nuclease on the extent of ejection from phage  $\lambda$ . *J. Phys. Chem. B.* 110:22261–22265.
15. Leforestier, A., and F. Livolant. 2009. Structure of toroidal DNA collapsed inside the phage capsid. *Proc. Natl. Acad. Sci. USA.* 106:9157–9162.
16. Jeembaeva, M., M. Castelnovo, F. Larsson, and A. Evilevitch. 2008. Osmotic pressure: resisting of promoting DNA ejection from phage  $\lambda$ . *J. Mol. Biol.* 381:310–323.
17. Cremer, T., and C. Cremer. 2001. Chromosome territories, nuclear architecture and gene regulation in mammalian cells. *Nat. Rev. Genet.* 2:292–301.
18. Cunha, S., T. Odijk, E. Süleymanoglu, and C. L. Woldringh. 2001. Isolation of the *Escherichia coli* nucleoid. *Biochimie.* 83:149–154.
19. Marenduzzo, D., C. Micheletti, and E. Orlandini. 2010. Biopolymer organization upon confinement. *J. Phys. Condens. Matter.* 22:283102.
20. Boulanger, P., M. le Maire, ..., L. Letellier. 1996. Purification and structural and functional characterization of FhuA, a transporter of the *Escherichia coli* outer membrane. *Biochemistry.* 35:14216–14224.
21. Leforestier, A., and F. Livolant. 2010. The bacteriophage genome undergoes a succession of intracapsid phase transitions upon DNA ejection. *J. Mol. Biol.* 396:384–395.
22. Leforestier, A., S. Brasilès, ..., F. Livolant. 2008. Bacteriophage T5 DNA ejection under pressure. *J. Mol. Biol.* 384:730–739.
23. Purohit, P. K., J. Kondev, and R. Phillips. 2003. Mechanics of DNA packaging in viruses. *Proc. Natl. Acad. Sci. USA.* 100:3173–3178.
24. Šiber, A., M. Dragar, ..., R. Podgornik. 2008. Packing nanomechanics of viral genome. *Eur. Phys. J. E.* 26:317–325.
25. Petrov, A. S., and S. C. Harvey. 2008. Packaging double-helical DNA into viral capsids: structures, forces, and energetics. *Biophys. J.* 95:497–502.
26. Raspaud, E., D. Durand, and F. Livolant. 2005. Interhelical spacing in liquid crystalline spermine and spermidine-DNA precipitates. *Biophys. J.* 88:392–403.
27. Strey, H. H., R. Podgornik, ..., V. A. Parsegian. 1998. DNA–DNA interactions. *Curr. Op. Struct. Biol.* 8:309–313.
28. Kanduč, M., A. Naji, ..., R. Podgornik. 2010. Dressed counterions: strong electrostatic coupling in the presence of salt. *J. Chem. Phys.* 132:124701–124715.
29. Lerman, L. S. 1971. A transition to a compact form of DNA in polymer solutions. *Proc. Natl. Acad. Sci. USA.* 68:1886–1890.
30. Maniatis, T., J. H. Venable, and L. S. Lerman. 1974. The structure of  $\psi$  DNA. *J. Mol. Biol.* 84:37–64.
31. Cohen, J. A., R. Podgornik, ..., V. A. Parsegian. 2009. A phenomenological one-parameter equation of state for osmotic pressures of PEG and other neutral flexible polymers in good solvents. *J. Phys. Chem. B.* 113:3709–3714.
32. Béalle, G., J. Jestinc, and D. Carrière. 2011. Osmotically induced deformation of capsid-like icosahedral vesicles. *Soft Matter.* 7:1084–1089.
33. Šiber, A., and R. Podgornik. 2009. Stability of elastic icosahedral shells under uniform external pressure: application to viruses under osmotic pressure. *Phys. Rev. E Stat. Nonlin. Soft Matter Phys.* 79:011919.
34. Evilevitch, A., J. W. Gober, ..., W. M. Gelbart. 2005. Measurements of DNA lengths remaining in a viral capsid after osmotically suppressed partial ejection. *Biophys. J.* 88:751–756.
35. São-José, C., M. de Frutos, ..., P. Tavares. 2007. Pressure built by DNA packing inside virions: enough to drive DNA ejection *in vitro*, largely insufficient for delivery into the bacterial cytoplasm. *J. Mol. Biol.* 374:346–355.
36. Ubbink, J., and T. Odijk. 1996. Deformation of toroidal DNA condensates under surface stress. *Europhys. Lett.* 33:353–358.
37. Landau, L. D., and E. M. Lifshitz. 1980. *Statistical Physics.*, Vol. 1. Pergamon Press, Oxford.
38. Tzllil, S., J. T. Kindt, ..., A. Ben-Shaul. 2003. Forces and pressures in DNA packaging and release from viral capsids. *Biophys. J.* 84:1616–1627.
39. Kanduč, M., A. Naji, ..., R. Podgornik. 2010. Dressed counterions: strong electrostatic coupling in the presence of salt. *J. Chem. Phys.* 132:124701–124715.
40. Rau, D. C., and V. A. Parsegian. 1992. Direct measurement of the intermolecular forces between counterion-condensed DNA double helices. Evidence for long range attractive hydration forces. *Biophys. J.* 61:246–259.
41. Rau, D. C., and V. A. Parsegian. 1992. Direct measurement of temperature-dependent solvation forces between DNA double helices. *Biophys. J.* 61:260–271.
42. Ben-Yaakov, D., D. Andelman, ..., R. Podgornik. 2009. Beyond standard Poisson-Boltzmann theory: ion-specific interactions in aqueous solutions. *J. Phys. Condens. Matter.* 21:424106.
43. Kanduč, M., A. Naji, ..., R. Podgornik. 2009. The role of multipoles in counterion-mediated interactions between charged surfaces: strong and weak coupling. *J. Phys. Condens. Matter.* 21:424103.
44. Fang, Y., and J. H. Hoh. 1998. Surface-directed DNA condensation in the absence of soluble multivalent cations. *Nucleic Acids Res.* 26:588–593.
45. Kato, A., E. Shindo, ..., K. Yoshikawa. 2009. Conformational transition of giant DNA in a confined space surrounded by a phospholipid membrane. *Biophys. J.* 97:1678–1686.
46. Parsegian, V. A., R. P. Rand, and D. C. Rau. 1995. Macromolecules and water: probing with osmotic stress. *Methods Enzymol.* 259:43–94.
47. Helgstrand, C., W. R. Wikoff, R. L. Duda, R. W. Hendreix, J. E. Johnson, and L. Liljas. 2003. The refined structure of a protein catenane: the HK97 bacteriophage capsid at 3.44 Å resolution. *J. Mol. Biol.* 334:885–899.
48. Effantin, G., P. Boulanger, ..., J. F. Conway. 2006. Bacteriophage T5 structure reveals similarities with HK97 and T4 suggesting evolutionary relationships. *J. Mol. Biol.* 361:993–1002.